SAND2017-11536C

Dynamic Measurements on Miniature Springs for Flaw and Damage Detection

Daniel P. Rohe
Structural Dynamics Department
Sandia National Laboratories*
P.O. Box 5800 - MS0557
Albuquerque, NM, 87185
dprohe@sandia.gov

ABSTRACT

Small components are becoming increasingly prevalent in today's society. Springs are a commonly found piece-part in many mechanisms, and as these components become smaller, so do the springs inside of them. Because of their size, small manufacturing defects or other damage to the spring may become significant: a tiny gouge might end up being a significant portion of the cross-sectional area of the wire. However, their small size also makes it difficult to detect such flaws and defects in an efficient manner. This work aims to investigate the effectiveness of using dynamic measurements to detect damage to a miniature spring. Due to their small size, traditional instrumentation cannot be used to take measurements on the spring. Instead, the non-contact Laser Doppler Vibrometry technique is investigated. Natural frequencies and operating shapes are measured for a number of springs. These results are compared against springs that have been intentionally flawed to determine if the change in dynamic properties is a reasonable metric for damage detection.

Keywords: SLDV, Damage Detection, Modal

1 INTRODUCTION

Small parts find their way into a number of components, especially in today's world of miniaturization. If such parts are involved in a system critical application, they often undergo some form of acceptance testing in order to determine whether or not there has been any damage or manufacturing defect prior to being installed. The component of interest in this work is a small extension spring, shown in Figure 1 laid on top of a penny for size reference. The spring itself is very small, a nick or gouge could easily penetrate a significant portion of the cross sectional area of the wire which could lead to decreased strength or fatigue life of the component. Unfortunately, the size and shape of the spring are not conducive to easy identification of such flaws. They would not be visible without the aid of magnifying optics, and the helical shape ensures that there are a number of hidden surfaces where such a flaw might be overlooked. Sandia National Laboratories has investigated many approaches to determining flaws in these objects including optical methods such as high-resolution microscopy, stiffness screening, digital radiography and computed tomography, electrical resistivity measurements, and thermal imaging during electrical conduction. None of these approaches yielded an efficient, robust way to identify damage to these parts.

* Sandia National Laboratories is a multimission laboratory managed and operated by National Technology and Engineering Solutions of Sandia LLC, a wholly owned subsidiary of Honeywell International Inc. for the U.S. Department of Energy's National Nuclear Security Administration under contract DE-NA0003525.

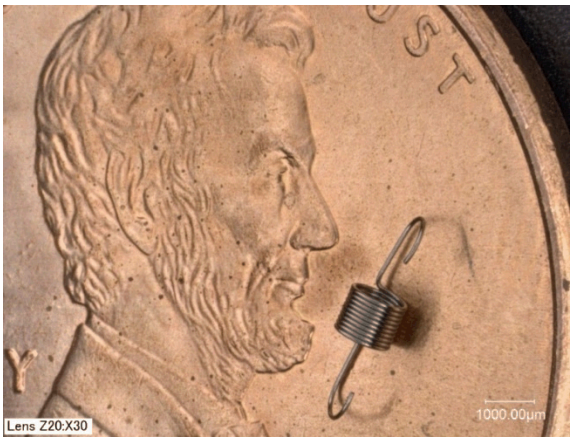

Figure 1: Small spring shown on an penny for size reference.

It is well known that damage to a particular component can influence a part's dynamic properties [1], so this work aimed to investigate whether such techniques could be used for these small springs. These parts have many properties that could confound a damage detection scheme. As this spring is at the lower size limit of what the manufacturer can produce reliably, there is significant amount of unit-to-unit variability between springs even within the same lot. There is also uncertainty in the boundary conditions during dynamic tests as the spring hooks are not always in the same plane, which results in different contact areas on the mounting pins. Additionally, the size of the spring poses challenges for excitation and data acquisition which can lead to reduced data quality.

Due to their size, accelerometers could not be adhered to the springs without significantly altering its mass and stiffness, and this would certainly derail any attempt to detect damage in the spring. Instead, a scanning laser Doppler vibrometer (SLDV) was used to measure the response of the spring to vibration excitation. The SLDV has advantages over traditional mounted sensors in that it does not mass load the test article. In addition, its sensor footprint is very small, so it can measure the motion of individual coils of the spring resulting in better mode shape resolution [2]. The natural frequencies and deflection shapes of several modes were extracted using the SLDV.

2 SPRING DYNAMIC TESTING

The spring is much smaller than the objects usually tested in the modal laboratory at Sandia National Laboratories. The wire diameter of the spring was approximately 75 µm, and the stretched length of the spring was about 0.5 cm. The mass of the spring was approximately 2 mg. Given that the smallest accelerometer owned by the modal laboratory at Sandia National Laboratories was over 100 times as massive as the spring, and any fixture onto which the accelerometer could be mounted would likely be equally as massive, the approach of identifying spring natural frequencies by measuring on the fixture itself was discarded. Instead, the laser vibrometer system would be used to measure directly on the spring itself.

A simple fixture was designed to hold the spring during testing, as shown in Figure 2. The fixture consisted of a rectangular base with two cylindrical pins. The fixture was excited using base excitation from a modal shaker (B+K Type 4809). In order to determine whether fixture modes would contaminate the spring data, preliminary finite element analysis of the fixture was performed, showing the first mode of the fixture above 100 kHz. This was well above the bandwidth of interest for the test so for this work the fixture was assumed to be rigid. Rather than trying to measure the force applied to the fixture by the shaker, a transmissibility approach was used instead. A reference accelerometer was mounted to the shaker alongside the fixture to serve as the input acceleration.

The SLDV was set up in 1D mode with a single laser head. A 3D measurement was initially considered to get the in-plane responses; however, it was unclear whether the laser system would be accurate enough to triangulate three laser points onto the thin wire of the spring. In the author's experience the typical alignment accuracy for the laser system is on the order of 0.1 to 0.5 mm, which is larger than the wire diameter. Additionally, only one set of close-up hardware (close-up module and lenses) were available to use at the time. Once testing started, it became clear that it would be useful to have an in-plane measurement to help identify the many modes in the bandwidth, but it was found that re-mounting the spring so the perpendicular face would be visible to the laser would result in changing natural frequencies. An alternative would be to move the laser head, but this would require re-aligning the laser to the part. Because a large number of springs were to be tested, this idea was discarded. Instead, a small piece of first-surface mirror was placed next to the spring on the shaker at a

45 degree angle allowing the laser system to measure two perpendicular sides of the spring. The final test setup can be seen in Figure 3. A representative view from the laser system is shown in Figure 4.

The SLDV was set up to measure 21 points on each face of the spring. This was supplemented by measurement points on the fixture to verify that it was in fact moving rigidly over the bandwidth of interest. For each test the transfer function between these fixture points and the reference accelerometer was verified to be close to 1. Because the spring is small and the laser spot is relatively bright, it was difficult to determine exactly where the laser spot was on the spring. To aid in finding the laser spot, an external camera was used to view the spring close up, and the video was sent to a large monitor. A ring light was used to brighten the test setup, equalizing the video image exposure between the bright laser spot and the relatively dark surrounding image. This setup is shown in Figure 5.

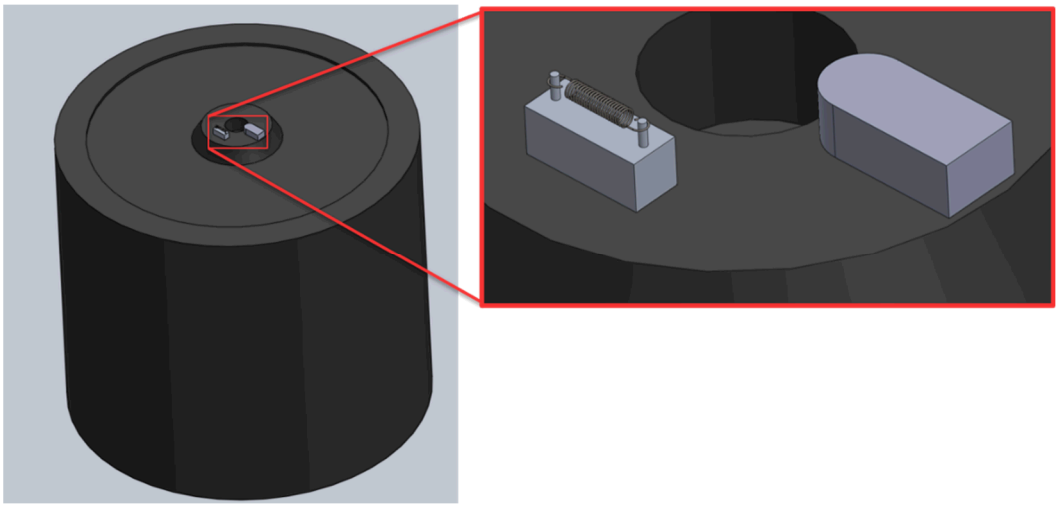

Figure 2: Schematic test setup showing the B&K Type 4809 shaker, spring fixture with spring, and a reference accelerometer.

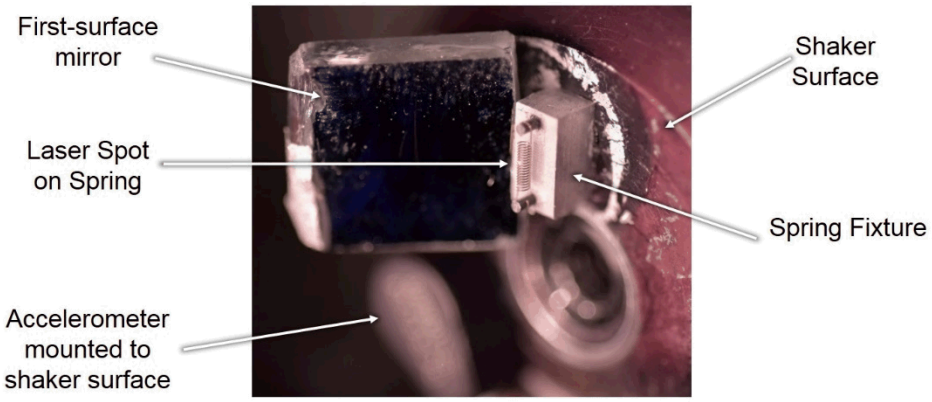

Figure 3: Close-up of test setup showing a spring mounted on the fixture alongside a first surface mirror that enables measurement of in-plane velocity.

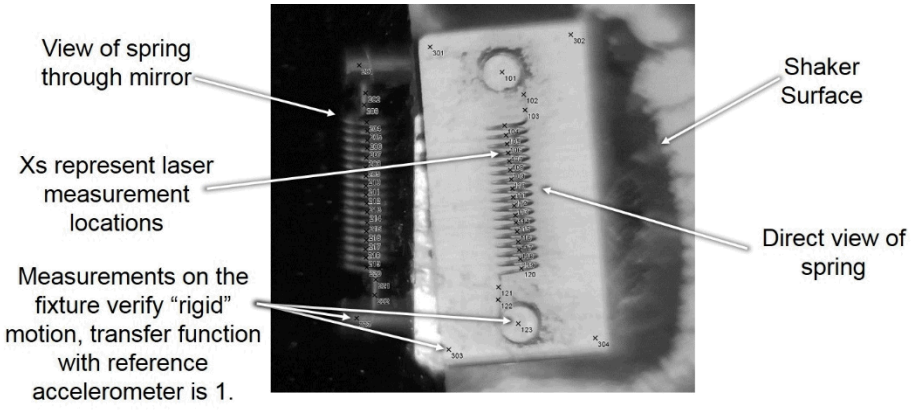

Figure 4: Representative view from the laser system; the spring can be seen directly on the right, but it can also be seen through the mirror on the left, which allows measuring the in-plane motions.

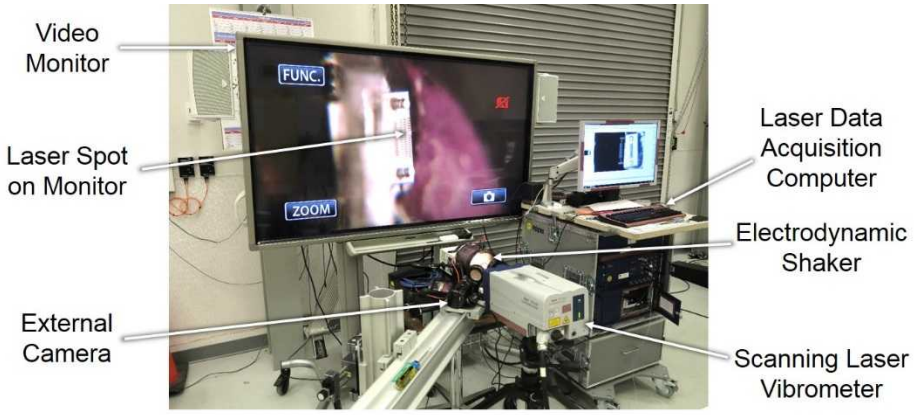

Figure 5: Overview of test setup showing the laser vibrometer, shaker, and video monitor used to find the laser spot.

Flat pseudorandom vibration was applied to the shaker, and the laser vibrometer measured responses on the spring and fixture. Reasonable laser signal quality was obtained with no surface preparation, though small changes in the position of the laser spot could result in large differences in signal quality due to the cylindrical shape of the wire. The measured degrees of freedom allowed most modes of interest to be spatially distinguished, with torsion being the exception; the single line of measurement points along the centerline of the spring did not adequately capture torsional motion. The in-plane modes were excited less strongly due to being perpendicular to the motion of the shaker. In addition, the asymmetric (2^{nd} and 4^{th}) bending modes were not excited well since both pins are nominally moving in the same direction, although they were generally still visible above the noise floor of the measurement.

3 NATURAL FREQUENCY DISTRIBUTIONS

Since the goal of this effort was to determine the health of springs, a distribution of unflawed natural frequencies was desired against which potentially flawed springs could be compared. In order to generate these distributions, a statistically significant number of tests needed to be performed. Seven healthy springs were available to generate these distributions, and each spring was tested four times (removing it from the pins and remounting it between each test). Figure 6 shows a complex mode indicator function (CMIF) that highlights the spread in natural frequencies observed by mounting one spring four different times. This spread can be attributed primarily to the boundary conditions of the spring; the spring, while placed on the pins as accurately as the test engineer's dexterity would allow, could potentially have one hook slightly higher on the pin than the other, resulting in a slightly longer stretched length. Additionally, due to manufacturing variability, many springs did not have their hooks exactly in the same plane, and this could result in one or both hooks contacting the pin in more than one location. Figure 7 shows the CMIF for each test of all unflawed springs.

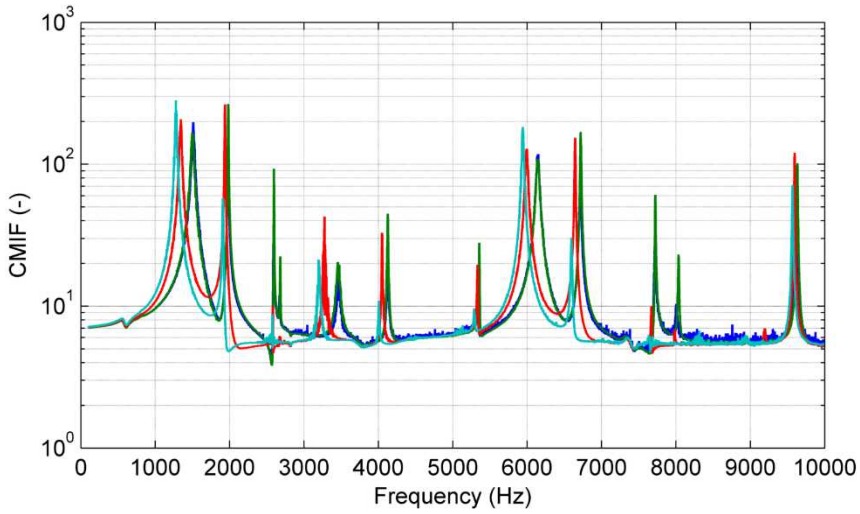

Figure 6: Spread in natural frequencies achieved by testing one spring four times.

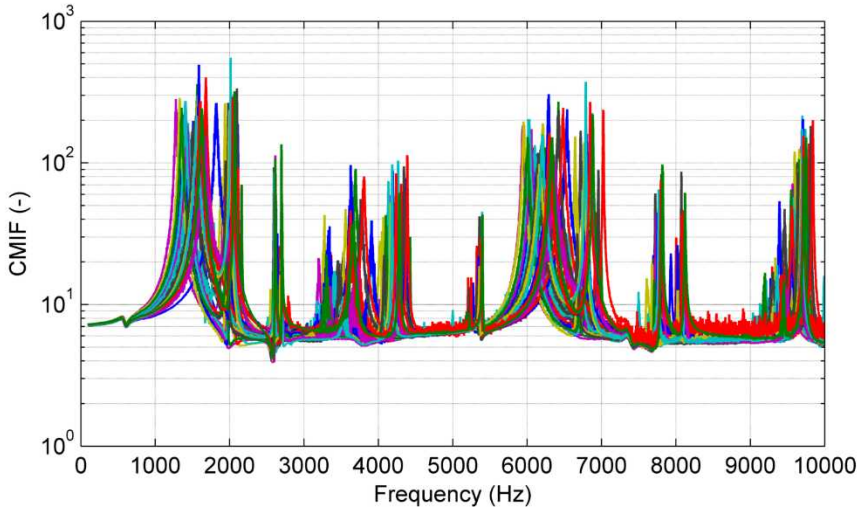

Figure 7: Spread in natural frequencies for all tests of all springs.

The prominent peaks in the CMIF in Figure 7 were then grouped by shape. The modes never switched order from spring to spring, which made this process easier (i.e. the first peak was always first bending mode in the out-of-plane direction, second peak was always first bending in the in-plane direction, etc.). A normal distribution was fit to the natural frequencies of each mode. Figure 8 shows this analysis for the first bending mode of the spring. Table 1 shows the natural frequencies for each spring as well as the mean and standard deviation for each mode. Some modes were grouped fairly tightly, with a standard deviation of less than 20 Hz, while others showed a larger spread with a standard deviation of almost 200 Hz.

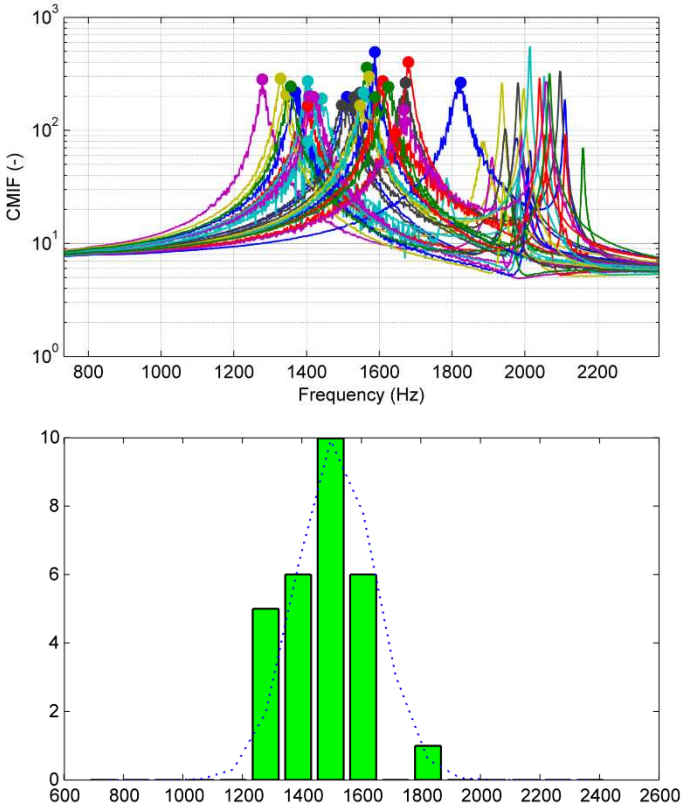

Figure 8: First mode peaks picked off CMIFs (top) and corresponding normal distribution (bottom).

Table 1: Healthy spring natural frequencies. (-- indicates mode not found in data).

	Mode 1	Mode 2	Mode 3	Mode 4	Mode 5	Mode 6	Mode 7	Mode 8	Mode 9	Mode 10	Mode 11	Mode 12	Mode 13
Spring 1 Test 1	1511	1978	2592	2669	3467	4122	5334	6150	6713	7716	8006	9197	9613
Spring 1 Test 2	1497	1981	2595	2680	3456	4125	5355	6141	6719	7722	8034	--	9633
Spring 1 Test 3	1344	1938	2580	--	3277	4048	5330	5989	6644	7670	7983	9195	9595
Spring 1 Test 4	1278	1909	2573	--	3195	4006	5288	5941	6595	7633	8316	--	9569
Spring 2 Test 1	1403	--	--	--	3902	--	--	6088	6556	--	--	9203	9577
Spring 2 Test 2	1403	2055	2600	2667	3364	4247	5323	6095	6838	7733	8003	9292	9695
Spring 2 Test 3	1566	2159	2617	2695	3694	4425	5380	6419	6997	7823	8122	9548	9756
Spring 2 Test 4	1369	2014	2588	2641	3344	4192	5272	6075	6797	7695	7931	9272	9680
Spring 3 Test 1	1547	1981	2589	--	3528	4138	5331	6188	6752	7698	8000	9328	9697
Spring 3 Test 2	1572	1881	2588	--	3558	4023	--	6211	6653	7608	--	9336	9650
Spring 3 Test 3	1408	1988	2592	2680	3331	4142	5345	6044	6748	7700	8008	9223	9684
Spring 3 Test 4	1442	2053	2608	2691	3408	4264	5378	6103	6873	7766	8088	9261	9739
Spring 4 Test 1	1645	2070	2614	2683	3747	4305	5353	6372	6920	7788	8066	9431	9791
Spring 4 Test 2	1588	2000	2602	2684	3586	4197	5352	6234	6813	7742	8025	9316	9750
Spring 4 Test 3	1823	2109	2622	2684	3909	4363	5358	6538	6969	7814	8072	9548	9811
Spring 4 Test 4	1672	2097	2617	2686	3761	4342	5359	6423	6956	7805	8072	9459	9811
Spring 5 Test 1	1328	1941	2594	2663	3252	4067	5295	5950	6673	7678	7923	9153	9656
Spring 5 Test 2	1419	1991	2613	--	3355	4145	5350	6058	6745	7733	8013	9245	9692
Spring 5 Test 3	1403	1981	2606	--	3333	4134	5345	6017	6741	7714	--	9213	9700
Spring 5 Test 4	1680	2113	2636	2698	3806	4388	5372	6484	7022	7850	8080	9559	9841

Spring 6 Test 1	1356	1958	2583	2663	3300	4098	5330	6005	6705	7708	--	9197	9655
Spring 6 Test 2	1588	2008	2598	2672	3628	4192	5342	6289	6803	7755	8019	9391	9706
Spring 6 Test 3	1530	1945	2583	2663	3484	4077	5325	6150	6673	--	--	9303	9638
Spring 6 Test 4	1547	1997	2594	2680	3513	4169	5358	6163	6767	7744	8022	9314	9683
Spring 7 Test 1	1667	2059	2614	2708	3683	4261	5400	6356	6847	7814	8108	9494	9686
Spring 7 Test 2	1556	2014	2603	2705	3523	4184	5395	6203	6788	7767	8089	9363	9697
Spring 7 Test 3	1609	2041	2609	2700	3625	4238	5386	6297	6845	7795	8100	9420	9714
Spring 7 Test 4	1625	2067	2613	2706	3675	4283	5398	6339	6881	7816	8122	9450	9723
Mean Value	1513	2012	2601	2682	3525	4192	5348	6190	6787	7742	8052	9335	9694
Standard Deviation	130	66	15	17	198	111	32	165	119	61	79	122	69

4 FLAWED SPRING DETECTION

In order to test whether or not the spring flaws could be detected by changes in natural frequency, a batch of healthy springs were deliberately flawed. A focused ion beam was used to create a cut in five springs approximately half the wire diameter deep in various locations. An additional spring was plastically yielded as a second form of damage to investigate. The six flawed springs were mixed with three healthy springs to perform a kind of "semi-blind" study to see if the flawed springs could be identified without *a priori* knowledge of which were flawed, which could bias the judgement of the technique. It should be noted that the author coordinated the flawing of the springs so he knew ahead of time how many flawed springs there were, but not which ones were flawed, which may bias the results.

To determine which springs were flawed, natural frequencies of this new batch were compared against the distributions from the unflawed baseline data in Table 1. Comparison of a measured natural frequency to its corresponding unflawed baseline distribution establishes the likelihood of that measurement if the spring were unflawed. If a natural frequency is unlikely to be found in the healthy distribution, it suggests the spring is in some way damaged. For each measured natural frequency, the percentage of the distribution that was farther from the mean than the given natural frequency was computed. Figure 10 through Figure 18 show the CMIFs from each of the blind test springs. The healthy natural frequency distributions are shown as vertical grey bands. Peaks corresponding to natural frequencies where the percentage of the distribution farther from the mean was less than 10% are annotated.

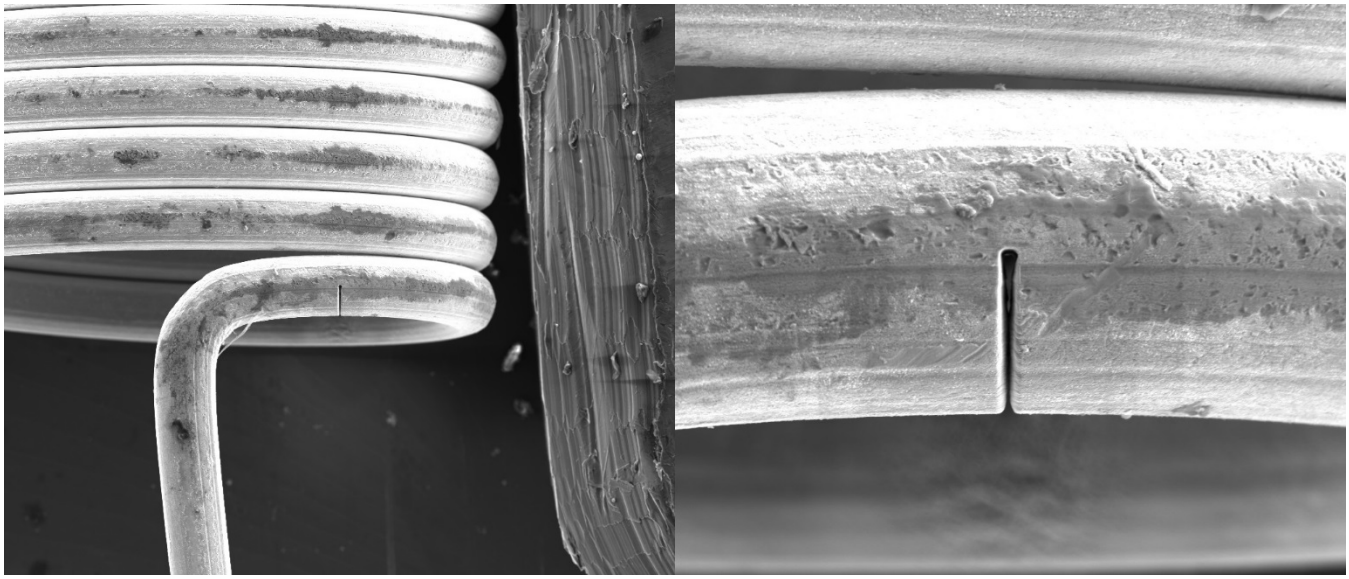

Figure 9: Flawed spring with a focused ion beam cut.

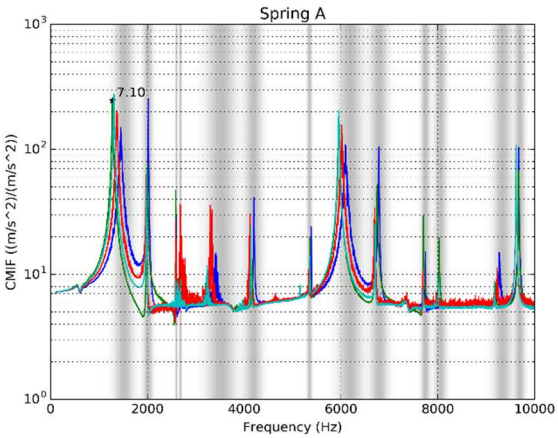

Figure 10: Spring A CMIFs

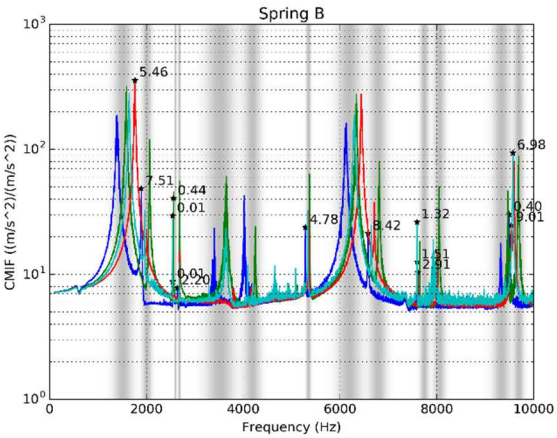

Figure 11: Spring B CMIFs

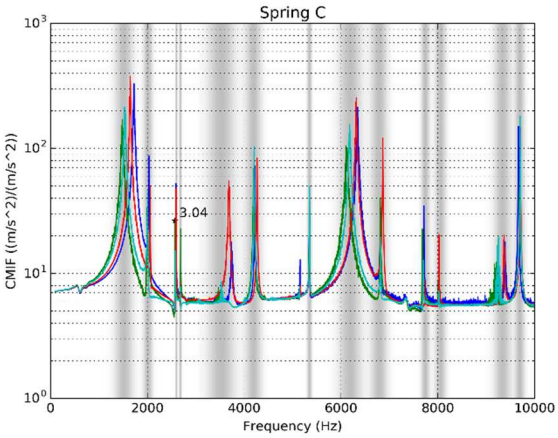

Figure 12: Spring C CMIFs

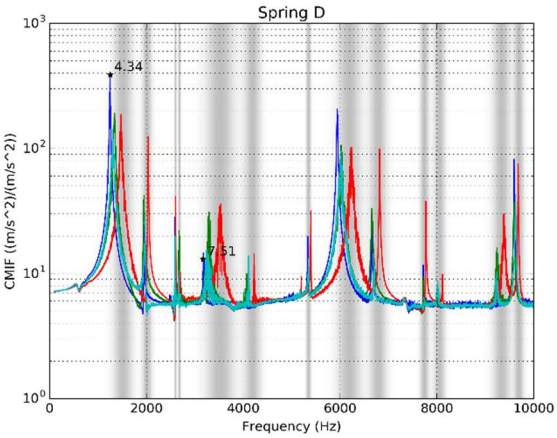

Figure 13: Spring D CMIFs

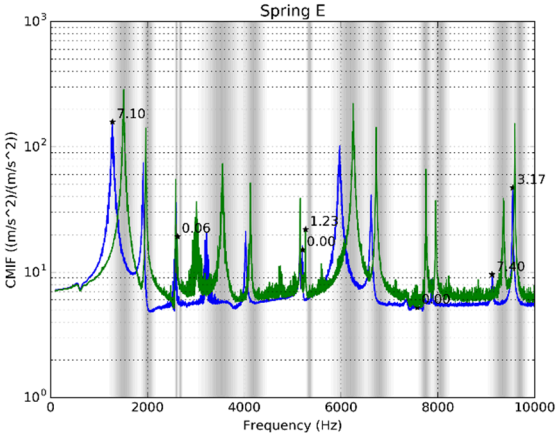

Figure 14: Spring E CMIFs

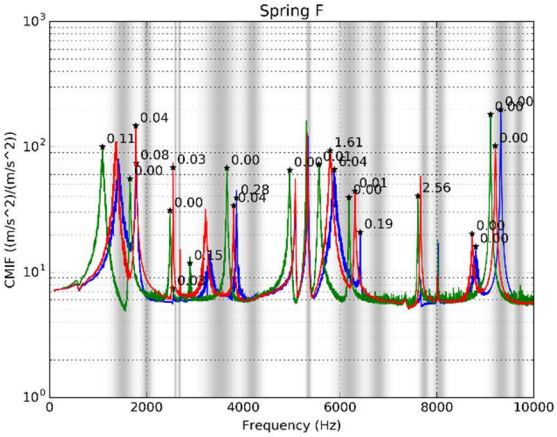

Figure 15: Spring F CMIFs

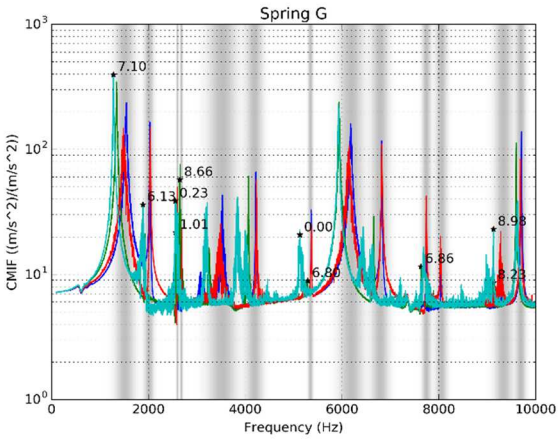

Figure 16: Spring G CMIFs

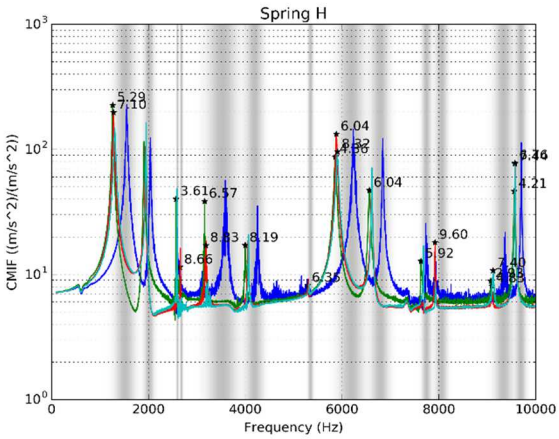

Figure 17: Spring H CMIFs

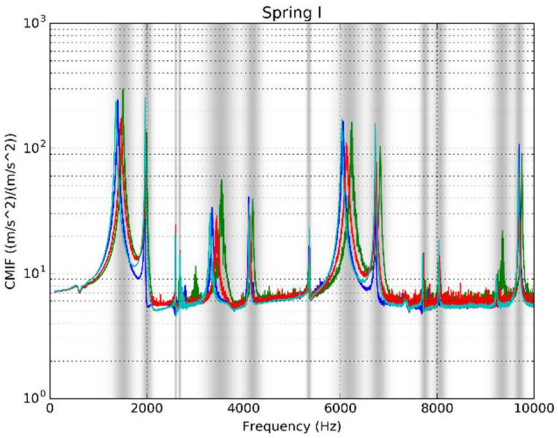

Figure 18: Spring I CMIFs

Springs B, E, F, G, and H contain the most peaks highlighted by the 10% metric. Spring F showed the most severe deviations from the healthy distributions. Spring E broke halfway through the testing with only two of four tests completed (it turns out that a spring breaking as it is being mounted is a great indication that it had some kind of damage!). Springs A, C, D, and I had the fewest peaks highlighted by the 10% metric. Spring I had all of its peaks well within the healthy spring distributions. Although we knew prior to this analysis that we should have at most three healthy springs, four of them (A, C, D, or I) did not generate high damage metrics by our method, so all were guessed to be healthy. This was thought to be fair as in practice an analyst would not have *a priori* knowledge of how many damaged springs they would have. Table 2 shows the blind predictions compared to the actual state of the springs. Three of nine assessed states were incorrect, which is not outstanding, especially considering two of the incorrect assessments are non-conservative in the sense that they would accept a flawed article.

Table 2: Results of blind identification of flaws based on outlier natural frequencies

Spring Letter	Our Guess?	Actual Flaw
A	**Healthy**	**FIB cut, 5 coils from hook, out of hook plane**
B	Flaw	FIB cut, 6 coils from hook, out of hook plane
C	Healthy	Healthy
D	**Healthy**	**FIB cut, 6 coils from hook, out of hook plane**
E	Flaw	FIB cut, 6 coils from hook, in hook plane
F	Flaw	Yielded Spring
G	**Flaw**	**Healthy**
H	Flaw	FIB cut, End coil next to hook

I	Healthy	Healthy

The data were re-examined (now with independent knowledge of which springs were actually healthy and which were flawed) to determine where potential oversights in the blind test occurred. On spring G (Figure 16), it was noted that the majority of the unlikely natural frequencies were found in the fourth test, and this test seemed to have a large amount of noise as shown by the CMIF. In the author's experience with these springs, the increased noise could suggest that the spring was not seated quite right on the pins of the fixture, which could result in the spring sliding or banging on the pin, and might also result in changing natural frequencies. The discarding of a healthy spring is perhaps not as severe of an issue as the acceptance of a flawed spring, however. Spring A and D both show only one or two unlikely natural frequencies, so this metric may not be suitable.

The mean first natural frequency of both spring A and D are over one standard deviation away from the mean of the healthy distribution, so this was investigated next. Bias in the mean value of the natural frequency for a given spring was examined for each mode of each spring. Table 3 shows the number of standard deviations of the spring's mean natural frequency was from the mean of the healthy distributions. Figure 19 shows the same values in graphical form. A trend can be observed where many of the flawed springs have mean natural frequencies lower than the healthy springs, and this is to be expected as all of the imposed flaws would tend to decrease stiffness and lower natural frequencies. However, there are clear exceptions to this rule. Spring B, for example, which is a flawed spring, has mean 1st, 8th, and 12th natural frequencies well over half a standard deviation higher than the healthy spring mean natural frequencies. If an analyst were rejecting springs simply on the basis of seeing a drop in natural frequency, spring B would be accepted while a healthy spring like spring G would be discarded as it has a number of mean natural frequencies that are well below the accepted healthy spring mean.

Table 3: Number of standard deviations of the spring mean from the healthy distribution mean. Flawed springs are shaded in grey.

	Mode 1	Mode 2	Mode 3	Mode 4	Mode 5	Mode 6	Mode 7	Mode 8	Mode 9	Mode 10	Mode 11	Mode 12	Mode 13
Spring A	-1.24	-0.28	-0.85	0.38	-1.06	-0.32	0.37	-1.12	-0.44	-0.55	-0.69	-1.04	-0.76
Spring B	0.63	-0.43	-3.57	-0.59	0.52	-0.54	-0.42	0.67	-0.85	-2.16	-0.77	0.79	-1.54
Spring C	0.62	0.17	-1.26	0.42	0.42	0.27	-0.05	0.27	0.34	-0.59	-0.44	-0.25	-0.05
Spring D	-1.32	-0.56	-0.48	-0.14	-1.08	-0.49	0.21	-0.83	-0.69	-0.11	-0.28	-0.38	-1.09
Spring E	-0.91	-1.09	-1.04	-3.44	-0.7	-1.03	-3.5	-0.48	-0.96	-0.2	-3.6	-0.82	-1.85
Spring F	-1.72	-4.07	-4.93	0.81	-1.94	-3.75	-4.34	-2.71	-4.07	-1.62	-0.43	-4.67	-7.06
Spring G	-0.77	-0.59	-1.57	-0.25	-0.77	-0.17	-1.89	-0.86	-0.2	-0.71	-0.19	-1.02	-0.62
Spring H	-1.27	-0.78	-0.99	-1.54	-1.18	-0.88	-1.41	-1.34	-1.08	-1.06	-1.64	-1.42	-1.38
Spring I	-0.6	-0.58	-0.58	0.05	-0.57	-0.51	0.24	-0.48	-0.31	-0.5	-0.17	-0.43	0.09

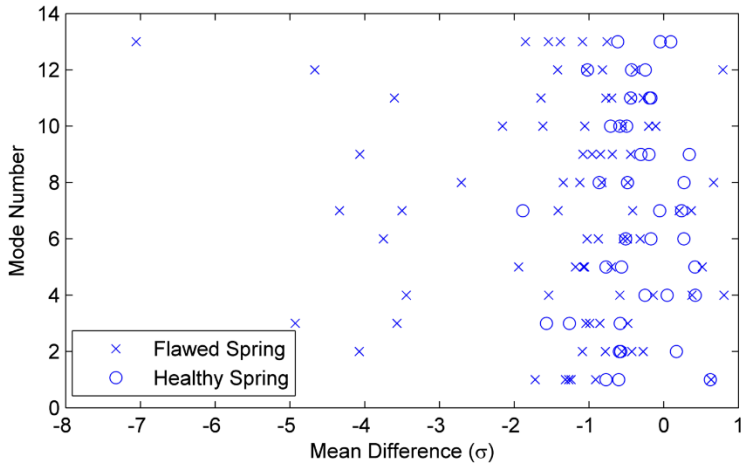

Figure 19: Number of standard deviations of the spring mean from the healthy distribution mean.

5 DISCUSSION

No definitive metric was found that correlated natural frequency to spring damage with 100% accuracy for the sample population of springs tested. Trends exist where the natural frequencies of damaged springs tend to be lower than those of healthy springs, but there are clear exceptions to this rule. The outlier frequency metric was able to correctly identify four of

six flawed springs, but also identified one healthy spring as flawed. The metric seemed to be more sensitive to damage due to yielding the springs (spring F) than those from nicks or cuts on the wire (which were fairly egregious reductions in the cross-sectional area of the springs).

One issue that is perhaps reducing the effectiveness of the technique is the spread of natural frequencies obtained. A large spread was found even when the same spring was tested multiple times, likely due to the boundary conditions of the spring, and this does not yet account for the significant manufacturing variability between different springs. The fixture could be improved so that there is a narrower range of positions that a spring could end up, perhaps by notching the pins rather than having them be smooth. More advanced tooling could also be created to aid the test engineer in placing the spring on the pins so the reliance on the engineer's manual dexterity to manipulate the very small objects could be reduced. It is thought that these improvements would potentially reduce the variability of the test setup and therefore allow the variability that is due to spring flaws to become more apparent.

A larger variety of flaws and higher population count to improve the baseline distributions could also be investigated. From the limited set, it is not clear whether a simple normal distribution or a more complex distribution is appropriate. Springs A, B, D, and E all had their flaws in approximately the same location on the spring. If local stiffness changes in this region do not result in natural frequency changes in the spring, then this effort may not have given the technique a fair trial.

Finally, a more sophisticated damage identification technique could be utilized that included shape information. The shapes achieved by this test were fairly noisy due to poor laser signal return at some points on the spring, so it was difficult to conclude whether a particular non-smooth part of the shape was due to a flaw or due to noise in the measurement. Photogrammetry/Digital Image Correlation is an alternative full-field technique that could be used to measure the motion of the spring with enough resolution to be able to identify local effects such as damage. The spring is likely too small to speckle appropriately for digital image correlation, but new techniques such as motion magnification [3,4] have shown promise in providing deflection shapes in applications similar to the one described here. Future work aims to investigate these techniques for determining flaws in these springs.

6 REFERENCES

[1] Doebling, S., Farrar, C., Prime, M., and Shevitz, D., "Damage Identification and Health Monitoring of Structural and Mechanical Systems from Changes in Their Vibration Characteristics: A Literature Review", Los Alamos National Laboratory Report LA-13070-MS, 1996.

[2] Castellini, P., Martarelli, M., and Tomasini, E.P., "Laser Doppler Vibrometry: Development of advanced solutions answering to technology's needs", *Mechanical Systems and Signal Processing*, Volume 20, Issue 6, p. 1265-1285, 2006.

[3] Dorn, Charles J., et al. "Automated extraction of mode shapes using motion magnified video and blind source separation." *Topics in Modal Analysis & Testing, Volume 10*. Springer, Cham, 2016. 355-360.

[4] Yang, Yongchao, et al. "Reference-free detection of minute, non-visible, damage using full-field, high-resolution mode shapes output-only identified from digital videos of structures." *Structural Health Monitoring,* 2017, 1475921717704385.